

# Broadband light generation at $\sim 1300$ nm through spectrally recoiled solitons and dispersive waves

Peter Falk,<sup>1</sup> Michael H. Frosz,<sup>1,2</sup> Ole Bang,<sup>1,\*</sup> Lars Thrane,<sup>1</sup> Peter E. Andersen,<sup>1</sup> Anders O. Bjarklev,<sup>1</sup> Kim P. Hansen,<sup>3</sup> and Jes Broeng<sup>3</sup>

<sup>1</sup>*DTU Fotonik, Department of Photonics Engineering, Technical University of Denmark, Building 343, DK-2800 Kgs. Lyngby, Denmark*

<sup>2</sup>*NKT Research and Innovation A/S, Blokken 84, DK-3460 Birkerød, Denmark*

<sup>3</sup>*Crystal Fibre A/S, Blokken 84, DK-3460 Birkerød, Denmark*

\*Corresponding author: bang@com.dtu.dk

Received November 13, 2007; accepted January 17, 2008;

posted January 31, 2008 (Doc. ID 89687); published March 14, 2008

We experimentally study the generation of broadband light at  $\sim 1300$  nm from an 810 nm Ti:sapphire femtosecond pump laser. We use two photonic crystal fibers with a second infrared zero-dispersion wavelength ( $\lambda_{Z2}$ ) and compare the efficiency of two schemes: in one fiber  $\lambda_{Z2} = 1400$  nm and the light at 1300 nm is composed of spectrally recoiled solitons; in the other fiber  $\lambda_{Z2} = 1200$  nm and the light at 1300 nm is composed of dispersive waves. © 2008 Optical Society of America

*OCIS codes:* 060.5295, 060.5530.

The dispersion of photonic crystal fibers (PCFs) can be significantly manipulated by changing the air hole structure in the cladding. Index-guiding PCFs can be designed to have a zero-dispersion wavelength down in the visible ( $\lambda_{Z1}$ ) and a second zero-dispersion wavelength ( $\lambda_{Z2}$ ) in the infrared, if desired. The combination of a small mode area and a tailored dispersion profile in so-called highly nonlinear PCFs has led to a revolution in supercontinuum generation (SCG) with low pump energies [1].

The nonlinear processes involved in SCG depend on the pumping scheme and are now generally well understood [2]. Supercontinuum light sources have become available commercially, and significant research is being aimed at improving the stability of the spectrum and tailoring the spectrum, e.g., to have increased bandwidth and power content in the blue [3] or wavelength regimes relevant for optical coherence tomography (OCT) [4,5], such as 800 or 1000 nm for ophthalmology (the eye) or 1300 nm for highly scattering tissue [6].

Here we focus on how to generate a broad, preferably Gaussian shaped, spectrum at  $\sim 1300$  nm. One way to generate power at 1300 nm is through degenerate four-wave mixing (FWM) of long pulses. However, FWM is typically inefficient, particularly if the Stokes wave is far from the pump [7]. Here we therefore consider how an 810 nm femtosecond (fs) pump can be used to generate a broad spectrum at  $\sim 1300$  nm.

One way to use a fs pump is to pump near  $\lambda_{Z1}$  in a conventional PCF with no  $\lambda_{Z2}$ , generate an octave spanning supercontinuum, and filter out the desired spectral part at  $\sim 1300$  nm with a Gaussian filter [8]. This scheme also has low efficiency. Another way is to pump sufficiently far into the anomalous regime to generate a single fundamental soliton and simultaneously avoid coupling too much energy into blue-shifted dispersive waves. Then let the soliton redshift

due to the Raman effect until it reaches the desired wavelength. This was, e.g., done in a tapered PCF where a 1300 nm pump was shifted to  $1.65 \mu\text{m}$  with 60% efficiency [9].

Recently there has been a lot of interest in pumping in the anomalous dispersion region in a PCF with two closely spaced zero-dispersion wavelengths [10–13]. In such fibers self-phase modulation (SPM) is dominant [11,12], which leads to a strong depletion of the pump over just a few centimeters and efficient generation of two smooth spectra in the normal dispersion region below  $\lambda_{Z1}$  and above  $\lambda_{Z2}$  [10–12].

Here we also use PCFs with two zero-dispersion wavelengths. However, because we want to transfer an 810 nm fs pump to 1300 nm, we need widely spaced zero-dispersion wavelengths [11,12,14], and therefore SPM is no longer the dominant effect. In such PCFs soliton fission generates solitons that redshift toward  $\lambda_{Z2}$ , where they generate dispersive waves in the normal regime above  $\lambda_{Z2}$  and thereby experience a spectral recoil that cancels the Raman redshift [15]. Several recoiled solitons might therefore accumulate below  $\lambda_{Z2}$  and transfer a significant amount of power to redshifted dispersive waves above  $\lambda_{Z2}$ . Depending on the fiber design, the power at 1300 nm could be made to consist of recoiled solitons or dispersive waves. The efficiency would, e.g., depend on the decay rate of the recoiled solitons, i.e., how much energy one soliton loses before the next one arrives. Here we experimentally compare the two schemes.

We study two highly nonlinear PCFs, NL-1.7-650 (fiber A) and NL-PM-760 (fiber N), fabricated by Crystal Fibre A/S. We measure the average hole diameter and pitch for the fibers from scanning electron microscopy (SEM) images and use these average dimensions to calculate the dispersion profiles numerically (see Fig. 1). Fiber A has zero dispersion at  $\lambda_{Z1} = 725$  nm and  $\lambda_{Z2} = 1390$  nm, whereas fiber N has

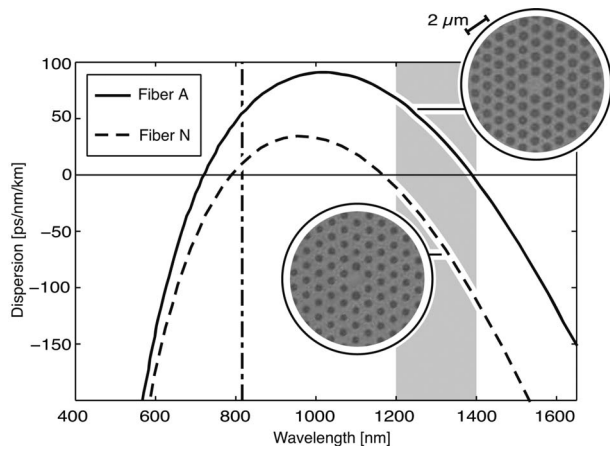


Fig. 1. Dispersion curves for fiber A (solid curve) and N (dashed curve) calculated from the inserted SEM images. Fiber A (N) has zero dispersion at  $\lambda_{Z1}=725$  nm (780 nm) and  $\lambda_{Z2}=1390$  nm (1170 nm). The pump wavelength is marked with a vertical dashed-dotted line.

zero dispersion at  $\lambda_{Z1}=780$  nm and  $\lambda_{Z2}=1170$  nm. Thus, fiber A has anomalous dispersion and fiber N has normal dispersion in the region of interest, 1200–1400 nm, marked as the gray area in Fig. 1.

The PCFs are pumped in the anomalous dispersion region by an 810 nm Ti:sapphire laser (FEMTOSOURCE Compact PRO, FEMTOLASERS) with a FWHM spectral bandwidth of 130 nm and a repetition rate of 75 MHz. The laser gives a transform-limited pulse length of 11.4 fs, which, due to the lenses in our setup, results in weakly positively chirped pulses at the fiber input with a FWHM of 21 fs. The coupling loss into the fiber is 3–4 dB minimum. In Fig. 2 we show the output spectra for different input powers. Up to 80% of the power is initially lost to blueshifted dispersive waves in the normal regime below  $\lambda_{Z1}$ , which is unwanted for the power-transfer schemes we investigate.

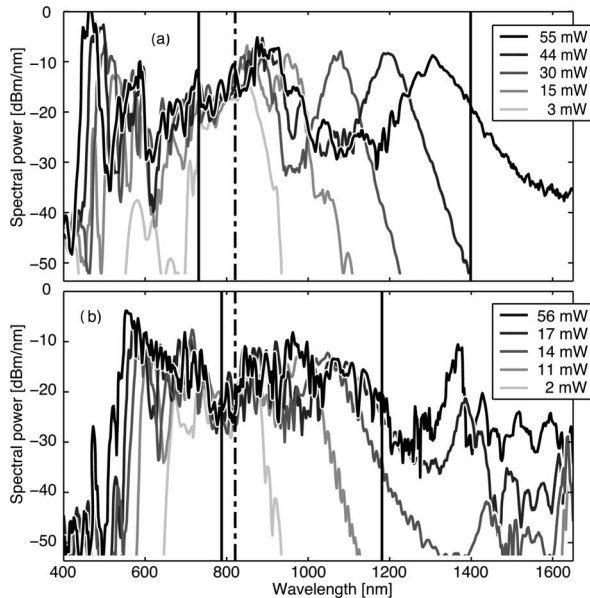


Fig. 2. Measured SCG from (a) 13.5 cm of fiber A and (b) 12.5 cm of fiber N for different average input powers. Zero-dispersion wavelengths (the pump) are marked by vertical solid (dashed-dotted) lines.

After the initial loss of energy to dispersive waves, the pump generates a number of solitons through soliton fission. The higher the input power is, the shorter the first generated lowest-order soliton will be and the more it will be redshifted after a fixed propagation length [2]. This is what is observed in Fig. 2. In fiber A we can clearly distinguish the lowest-order soliton for input powers above 30 mW. The first soliton has reached  $\lambda_{Z2}$  for an input power of  $\sim 55$  mW and has started to generate redshifted dispersive waves.

For fiber N with a significantly narrower anomalous dispersion regime, redshifted dispersive waves are generated already at 14 mW input power, and no individual solitons can be clearly distinguished. In fact, even for low pump powers, the spectrum develops into a broad supercontinuum, which is explained by the fact that fiber N is being pumped much closer to  $\lambda_{Z1}$ . For fiber N the second zero-dispersion wavelength therefore acts more as a limiter of the SCG, which could still be a desirable effect, nevertheless.

In Fig. 3 we show a contour plot of the measured output spectrum versus the input power for different fiber lengths. For fiber A we see that with only 6 cm of fiber one must pump with more than 55 mW for a soliton to reach  $\lambda_{Z2}$ , while a longer length of 180 cm allows more solitons to reach  $\lambda_{Z2}$ , the first one arriving above 15 mW and the second above 40 mW. It appears as if the first recoiled soliton loses most of its power before the second soliton arrives at  $\lambda_{Z2}$  (this will be quantified in the next figure). For fiber N Fig. 3 confirms again that the anomalous dispersion regime is so narrow and the effective nonlinearity so strong, that the solitons that are generated are spectrally too close to be clearly distinguished. For fiber A dispersive waves are generated at  $\sim 1500$  nm, and for fiber N they are generated at  $\sim 1300$  nm, as expected.

The power transfer for the two schemes may be quantified through the efficiency, calculated by numerically applying a 100 nm FWHM Gaussian filter centered at 1300 nm to the output spectrum and dividing by the input power. The efficiency is depicted

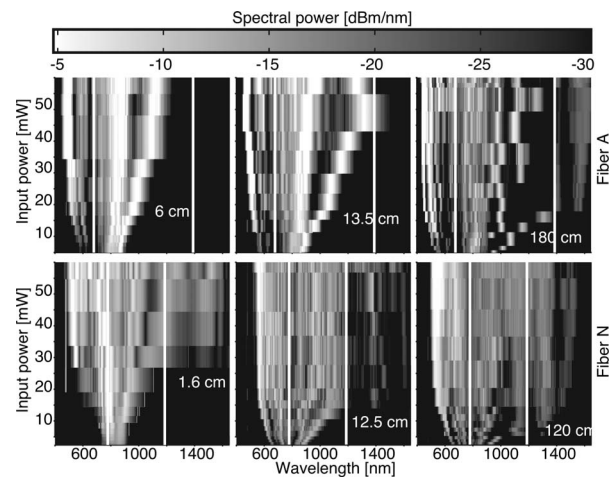


Fig. 3. Gray-scale contour plot of the average input power versus output spectrum of fibers A (top) and N (bottom) for different fiber lengths indicated on the figure. Zero-dispersion wavelengths are marked with white lines.

in Fig. 4 versus the input power for the three lengths of fiber. Naturally the efficiency will never be high due to the initial significant loss of power to blue-shifted dispersive waves below  $\lambda_{Z1}$ .

For fiber A (the soliton scheme) the measurement for 180 cm shows that unfortunately there is no accumulating effect for this fiber design. The recoiled soliton loses its power to redshifted dispersive waves before the next soliton arrives at  $\lambda_{Z2}$ . Note that the power in the next soliton at  $\sim 55$  mW is much less than the first soliton in accordance with the soliton fission theory [2]. For the shorter fiber lengths a higher input power is necessary for the first soliton to experience enough redshift to arrive at  $\lambda_{Z2}$ . Since the power predominantly goes into the first soliton, this means that the efficiency is higher. The largest efficiency for the soliton scheme is  $\sim 16\%$ , which is obtained for the 13.5 cm fiber.

For fiber N the scenario is much different. Clearly the dynamics is that of SCG and not single solitons arriving at  $\lambda_{Z2}$ . The efficiency increases initially with the input power, but above a certain saturation power, which depends on the fiber length, the supercontinuum has been generated completely, and there is no advantage in increasing the input power further. The saturation power is  $\sim 55$  mW for fiber lengths of 1.6 and 12.5 cm and  $\sim 15$  mW for 120 cm. Thus, above 55 mW, there is no point in increasing the fiber length. The maximum efficiency for this scheme is  $\sim 10\%$ .

In conclusion, we have experimentally investigated PCFs with two zero-dispersion wavelengths,  $\lambda_{Z1}$  and

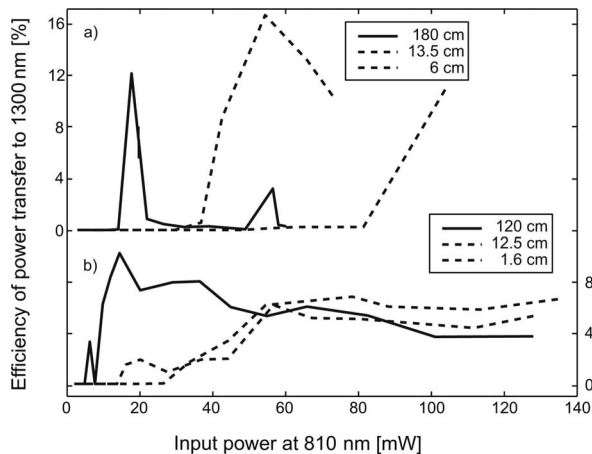


Fig. 4. Efficiency of the generation of power in the 1250–1350 nm regime calculated by filtering the output spectrum with a 100 nm FWHM Gaussian filter centered at 1300 nm and dividing the resulting filtered power with the total input power: (a) fiber A and (b) fiber N.

$\lambda_{Z2}$ , pumped at 810 nm in the anomalous regime with a fs laser. By using two PCFs with  $\lambda_{Z2}=1400$  and 1200 nm, respectively, we have been able to compare the efficiency of the transfer of power from 810 to 1300 nm for two schemes based on accumulating recoiled solitons and redshifted dispersive waves, respectively. We have shown that the rate of the power transfer from solitons to dispersive waves is too high for an accumulating effect to take place in the soliton scheme. The coupling efficiency to dispersive waves could possibly be reduced by appropriate dispersion design, which we leave for future work. We have also shown that in the dispersive wave scheme, because we pump closer to  $\lambda_{Z1}$ , the SCG process is too strong to observe isolated solitons arriving at  $\lambda_{Z2}$ . In this case the second zero-dispersion wavelength acts as a limiter for the strong SCG process. The two schemes have comparable efficiencies.

P. Falk acknowledges financial support from Danish Technical Research Council, grant 26-02-0020.

## References

1. J. K. Ranka, R. S. Windeler, and A. J. Stentz, *Opt. Lett.* **25**, 25 (2000).
2. J. M. Dudley, G. Genty, and S. Coen, *Rev. Mod. Phys.* **78**, 1135 (2006).
3. L. Tartara, I. Christiani, and V. Degiorgio, *Appl. Phys. B* **77**, 307 (2003).
4. A. D. Aguirre, N. Nishizawa, J. Fujimoto, W. Seitz, M. Lederer, and D. Kopf, *Opt. Express* **14**, 1145 (2006).
5. H. Wang and A. M. Rollins, *Appl. Opt.* **46**, 1787 (2007).
6. W. Drexler, *J. Biomed. Opt.* **9**, 47 (2004).
7. N. I. Nikolov, T. Sørensen, O. Bang, and A. Bjarklev, *J. Opt. Soc. Am. B* **20**, 2329 (2003).
8. I. Hartl, X. D. Li, C. Chudoba, R. K. Ghanta, T. H. Ko, J. G. Fujimoto, J. K. Ranka, and R. S. Windeler, *Opt. Lett.* **26**, 608 (2001).
9. X. Liu, C. Xu, W. H. Knox, J. K. Chandalia, B. J. Eggleton, S. G. Kosinski, and R. S. Windeler, *Opt. Lett.* **26**, 358 (2001).
10. K. M. Hilligsøe, T. V. Andersen, H. N. Paulsen, C. K. Nielsen, K. Mølmer, S. Keiding, R. Kristiansen, K. P. Hansen, and J. J. Larsen, *Opt. Express* **12**, 1045 (2004).
11. M. H. Frosz, P. Falk, and O. Bang, *Opt. Express* **13**, 6181 (2005).
12. M. H. Frosz, P. Falk, and O. Bang, *Opt. Express* **15**, 5262 (2007).
13. P. Falk, M. H. Frosz, and O. Bang, *Opt. Express* **13**, 535 (2005).
14. G. Genty, M. Lehtonen, H. Ludvigsen, and M. Kaivola, *Opt. Express* **12**, 3471 (2004).
15. D. V. Skryabin, F. Luan, J. C. Knight, and P. St. J. Russell, *Science* **301**, 1705 (2003).